Simultaneous electromagnetically induced transparency and absorption in thermal atomic medium

Shangqing Liang (梁尚清)[1], Yunfei Xu (徐云飞)[1], and Qiang Lin (林 强)[2,*]

[1]*Institute of Optics, Department of Physics, Zhejiang University, Hangzhou 310027, China*
[2]*Center for Optics & Optoelectronics Research, College of Science, Zhejiang University of Technology, Hangzhou 310023, China*
**Corresponding author: qlin@zju.edu.cn*

Received March 18, 2017; accepted May 25, 2017; posted online June 21, 2017

A three-level lambda system driven by multicolor control, pump, and probe fields is investigated. The pump and probe fields are derived from the same laser with opposite propagating directions. Due to the Doppler effect, the zero group-velocity atoms face bichromatic fields, while other atoms face trichromatic fields. The atomic medium shows distinct characteristics and exhibits simultaneous electromagnetically induced transparency (EIT) and electromagnetically induced absorption (EIA) at two frequencies. EIT and EIA peaks have a fixed relationship with frequency, which is determined by the Doppler shifts.

OCIS codes: 020.1670, 270.1670.
doi: 10.3788/COL201715.090201.

Electromagnetically induced transparency (EIT) or coherent population trapping (CPT, balance-EIT) remarkably reduces the atomic absorption[1,2], while electromagnetically induced absorption (EIA) enhances the absorption[3]. Obviously, they are the opposite effects in quantum optics. Since both of them have found a large amount of various applications, they have been extensively studied. They are both used to build a low power atomic clock, which is a very important application[4–7]. They have been used for magnetic field measurements. Both scalar and vector measurements can be implemented with EIT[8,9]. The relationship between the magnetic field and EIA has also been reported[10]. By greatly modifying the dispersion properties of an optical medium, EIT can slow light down and store the information of light into the atomic medium, which might be applied to quantum information, optical buffers in optical communication, precision measurements, and optical devices[1,11,12]. On the contrary, EIA can be used to prepare a fast light medium[13], which could have applications in a gyroscope[14].

It is convenient to achieve EIT by applying two coherent optical fields to a three-level system[1]. EIA could be found in a two-level degenerate system with the condition $F_e = F_g + 1$ (F_g and F_e are the total angular momentum of the ground and excited levels, respectively) satisfied[3]. A three-level lambda system interacting with three optical fields in an N configuration scheme can also exhibit EIA, which requires no more special conditions. In that case, EIA is obtained due to population transfer[15]. Two off-resonance fields transfer the atom population from the lower ground state to the upper ground state through a Raman process, and a third resonant probe field drives the transitions between the upper ground state and the excited state. Then, the high contrast EIA phenomenon is observed. However, simultaneous EIT and EIA have been less explored. EIT and Raman gain have been combined to create a different dispersion property in a medium for generating slow and fast light at the same time[16]. Three optical fields in an N configuration structure with a radio-frequency field could slow and accelerate light at the same time too[17]. Simultaneous EIT and EIA could be achieved in a similar way[18]. Multi processes could be generated by multicolor fields. Each process is formed with different fields, and there is no correlation among them, so this is a very simple way to achieve simultaneous EIT and EIA.

In this Letter, a kind of Doppler-induced EIT and EIA, which occur simultaneously, is demonstrated. The Doppler effect is involved in the coherent spectrum of a hot atomic medium, which is quite different from that in cold atoms[19–23]. The Doppler shifts must be considered when the interaction between atoms and optical fields is investigated. As shown in Fig. 1, it should be considered that a three-level atomic medium is irradiated by three

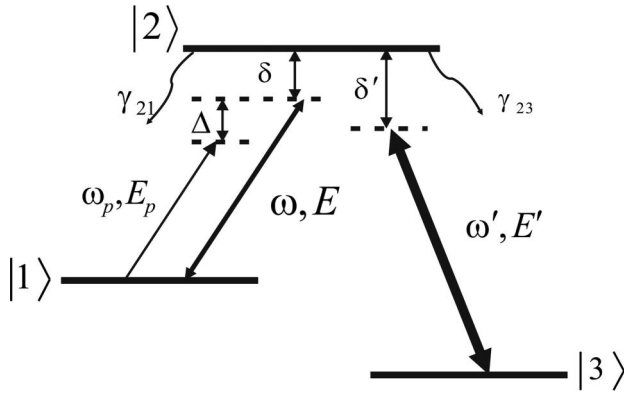

Fig. 1. Pump field and probe field drive the same transition $|1\rangle \rightarrow |2\rangle$, while the control field drives the transition $|3\rangle \rightarrow |2\rangle$. δ and δ' are the detuning from resonance. γ_{21} and γ_{23} are the decay rates.

optical fields. This system was studied by Berman and Xu, but the Doppler shift was not considered[24]. Here, adding the Doppler shift into their model, it is found that the system exhibits simultaneous EIT and EIA at two frequencies. The three optical fields are control field E', pump field E, and probe field E_p, respectively. E' drives transitions between energy levels $|2\rangle$ and $|3\rangle$ with angular frequency ω'. δ' is the coupling detuning and is defined as $\delta' = \omega_{23} - \omega'$. E drives transitions between energy levels $|2\rangle$ and $|1\rangle$ with angular frequency ω, and $\delta = \omega_{21} - \omega$ is the coupling detuning. E_p also drives transitions between energy levels $|2\rangle$ and $|1\rangle$ with angular frequency ω_p. $\Delta = \omega_p - \omega$ is the frequency difference between E_p and E. γ_{21} and γ_{23} are the decay rates from level $|2\rangle$ to $|1\rangle$ and to $|3\rangle$, respectively.

A particular situation is investigated here: the pump field and the probe field derive from the same laser system with opposite traveling directions. The two fields always have the same angular frequency when the frequency of the probe field is scanned. The control field travels along the direction of the probe field. Then, the optical fields are bichromatic for zero group-velocity atoms and trichromatic for other atoms. It plays different roles in the interaction of field and atoms and will be discussed later.

The density matrix solution obtained by Berman's mode is shown as follows. The electric field vectors of the pump field and the probe field are

$$\vec{E}(R,t) = \vec{E}\cos(\vec{k}\cdot\vec{R} - \omega t), \tag{1}$$

$$\vec{E}_p(R,t) = \vec{E}_p\cos(\vec{k}\cdot\vec{R} - \omega t). \tag{2}$$

The electric field vectors of the control field are

$$\vec{E}'(R,t) = \vec{E}'\cos(\vec{k}'\cdot\vec{R} - \omega' t). \tag{3}$$

The Hamiltonian for the atom-field system is

$$H = H_0 - \vec{\mu}\cdot[\vec{E}(\vec{R},t) + \vec{E}'(\vec{R},t) + E_P(\vec{R},t)], \tag{4}$$

where H_0 is the free-atom Hamiltonian, and μ is the atomic dipole moment operator. The density matrix in the Schrödinger picture, $\rho^s(t)$, characterizing this atom-field system evolves as

$$i\hbar\dot{\rho}_s = [H, \rho^s] + (\text{relaxation terms}). \tag{5}$$

A field interaction representation is introduced in which

$$\rho^s_{12} = \rho_{12}e^{-i(\vec{k}\cdot\vec{R} - \omega t)}, \tag{6a}$$

$$\rho^s_{32} = \rho_{32}e^{-i(\vec{k}'\cdot\vec{R} - \omega' t)}, \tag{6b}$$

$$\rho^s_{13} = \rho_{13}e^{-i[(\vec{k}-\vec{k}')\cdot\vec{R} - (\omega-\omega')t]}, \tag{6c}$$

$$\rho^s_{13} = \rho^{s*}_{13}. \tag{6d}$$

In the representation and in the rotating-wave approximation, one can write the time evolution equations for the density matrix elements in matrix form as

$$\dot{\rho} = -A\rho + B_+\rho e^{-i(\vec{k}_p - \vec{k}')\cdot\vec{R}e^{i\Delta t}} - B_-\rho e^{i(\vec{k}_p - \vec{k}')\cdot\vec{R}e^{-i\Delta t} + \lambda}, \tag{7}$$

with $\rho = [\rho_{11}, \rho_{13}, \rho_{31}, \rho_{12}, \rho_{21}, \rho_{32}, \rho_{23}, \rho_{22}]$ and $\lambda = [0,0,0,0,0,i\chi', -i\chi', 0]$, thus

$$A = \begin{pmatrix} 0 & 0 & 0 & -i\chi & i\chi & 0 & 0 & -\gamma_{2,1} \\ 0 & -i(\delta-\delta') & 0 & -i\chi' & 0 & 0 & i\chi & 0 \\ 0 & 0 & (\delta-\delta') & 0 & i\chi' & -i\chi & 0 & 0 \\ -i\chi & -i\chi' & 0 & \gamma - i\delta & 0 & 0 & 0 & i\chi \\ i\chi & 0 & i\chi' & 0 & \gamma + i\delta & 0 & 0 & -i\chi \\ i\chi' & 0 & -i\chi & 0 & 0 & \gamma - i\delta' & 0 & 2i\chi' \\ -i\chi' & i\chi & 0 & 0 & 0 & 0 & \gamma + i\delta' & -2i\chi' \\ 0 & 0 & 0 & i\chi & -i\chi & i\chi' & -i\chi' & \gamma_2 \end{pmatrix}, \tag{8}$$

$$B_+ = i\chi_p \begin{pmatrix} 0&0&0&0&1&0&0&0 \\ 0&0&0&0&0&0&-1&0 \\ 0&0&0&0&0&0&0&0 \\ 1&0&0&0&0&0&0&-1 \\ 0&0&0&0&0&0&0&0 \\ 0&0&1&0&0&0&0&0 \\ 0&0&0&0&0&0&0&0 \\ 0&0&0&0&1&0&0&0 \end{pmatrix}, \tag{9}$$

$$B_- = i\chi_p \begin{pmatrix} 0&0&0&1&0&0&0&0 \\ 0&0&0&0&0&0&0&0 \\ 0&0&0&0&0&1&0&0 \\ 0&0&0&0&0&0&0&0 \\ -1&0&0&0&0&0&0&1 \\ 0&0&0&0&0&0&0&0 \\ 0&-1&0&0&0&0&0&0 \\ 0&0&0&-1&0&0&0&0 \end{pmatrix}, \tag{10}$$

where $\chi = -\mu_{21}\cdot E/(2\hbar)$, $\chi' = -\mu_{31}\cdot E'/(2\hbar)$, $\chi_P = -\mu_{21}\cdot E_P/(2\hbar)$ are Rabi frequencies, γ_2 is the

excited-state decay rate resulting from spontaneous emission, $\gamma = \gamma_2/2$ is the decay rate of the optical coherences ρ_{12} and ρ_{32}. The probe light and the control light are copropagating. The probe light and the pump light are backpropagating.

One case is considered. The detuning of controlling is 60γ, and the frequencies of the probe light and pump light have the same value and are scanning at the same time. Considering the Doppler effects, the detuning of light can be rewritten as

$$\Delta = \omega_{p0}\left(1+\frac{v}{c}\right) - \omega_0\left(1-\frac{v}{c}\right) = \frac{2v}{c}\omega_0, \tag{11}$$

$$\delta = \omega_{21} - \omega = \omega_{21} - \omega_0\left(1-\frac{v}{c}\right), \tag{12}$$

$$\begin{aligned}\delta' = \omega_{23} - \omega' &= \omega_{23} - \omega_0'\left(1+\frac{\nu}{c}\right)\\ &= \omega_{23} - (\omega_{23} - 60\gamma)\left(1+\frac{\nu}{c}\right)\\ &= 60\gamma + (60\gamma - \omega_{23})\frac{\nu}{c},\end{aligned} \tag{13}$$

Δ is the detuning between the probe light and the pump light. δ is the detuning of the pump light, and δ' is the detuning of the controlling light.

A solution to these equations can be written in the form

$$\rho = \rho^{(0)} + \rho^{(+)} e^{-i(\vec{k}_p - \vec{k})\cdot\vec{R}e^{i\Delta t}} + \rho^{(-)} e^{i(\vec{k}_p - \vec{k})\cdot\vec{R}e^{-i\Delta t}}. \tag{14}$$

The probe absorption coefficient is proportional to $\alpha_p = -\mathrm{Im}[\gamma\rho_{12}^{(+)}/\chi_p]$. In the calculation, $\gamma_2 = 2\gamma_{21} = 2$ is the decay rate of the excited state, $\chi = 6\gamma_{21}$ and $\chi' = 10\gamma_{21}$ are the Rabi frequencies of E and E', respectively. The detuning $\delta' = \omega_{23} - \omega' = \pm 60\gamma_{21}$ is studied. The results are shown in Fig. 2.

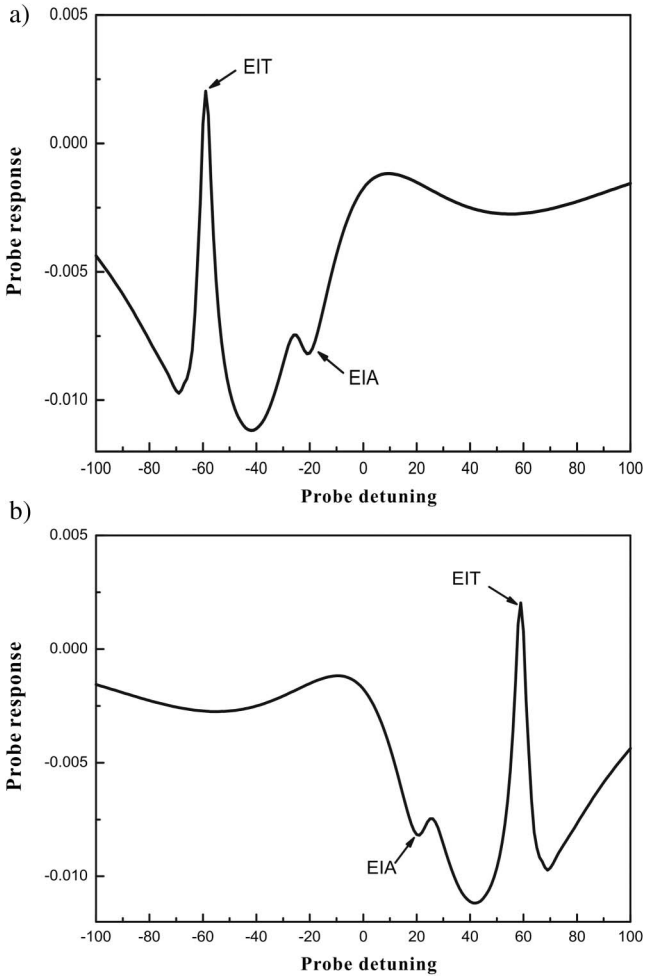

Fig. 2. Calculated probe response versus the probe detuning for $\gamma_{21} = \frac{\gamma_2}{2} = 1$, $\chi = 6\gamma_{21}$, and $\chi' = 10\gamma_{21}$. (a) $\delta' = \omega_{23} - \omega' = 60\gamma_{21}$, (b) $\delta' = \omega_{23} - \omega' = -60\gamma_{21}$.

It is obvious that the detuning frequency of the probe field for EIT is three times of that for EIA. It is interesting that the relationship still stays unchanged even when the detuning of the control field is tuned. This phenomenon can be explained with Doppler shifts. The frequency difference between $|1\rangle$ and $|3\rangle$ is defined as Δ_{hfs} and $\Delta_{\mathrm{hfs}} \ll \omega, \omega', \omega_p$. First, it focuses on the EIT signal at $-60\gamma_{21}$. The control field and the probe field form a typical EIT configuration in a three-level lambda system. When the two-photon detuning is zero, i.e., $\omega_p - \omega' = \Delta_{\mathrm{hfs}}$, the EIT signal is observed. As mentioned above, the velocity distribution of atoms would be considered. The zero group-velocity atoms, as shown in Fig. 3(a), face bichromatic fields. The pump field and the probe field have the same angular frequency. So, the pump field and the control light also satisfy the EIT condition. Other atoms then face trichromatic fields, as shown in Fig. 3(b). The single-photon detuning δ' changed with the Doppler shift. But the two-photon resonance condition is always satisfied. So, all the atoms contribute to the EIT signal. The pump field and the control field do not satisfy the two-photon resonance condition anymore. When the Doppler shift makes one velocity group of atoms resonate with the pump field, these atoms are pumped to the excited state. The absorption rate of the probe is then reduced. Since the probe field is off-resonant, this process is not a dominating one. But, it becomes a dominating process for EIA, which is shown later.

Next, it shows the reason why the EIA signal exists. The detuning of the control field is δ'. It should concentrate on the situation that the detuning of the probe field and the pump field are tuned to at $\delta'/3$, which is shown in Fig. 4(a). There is nothing special for the zero group-velocity atoms. If the velocity of the atoms is not zero, the Doppler shift should be considered. The difference between the Doppler shifts of the probe field and the control field is negligible, since $\Delta_{\mathrm{hfs}} \ll \omega', \omega_p$. If the shifts $\Delta\omega'$ and $\Delta\omega_p$ are positive, and $\Delta\omega' = \Delta\omega_p = \delta'/3$, the shift of the pump field is then $\Delta\omega = -\delta'/3$. It is obvious that the control field and the pump field interacting with these velocity group atoms satisfy the EIT condition. The probe field is resonant with these atoms to the moment, which is

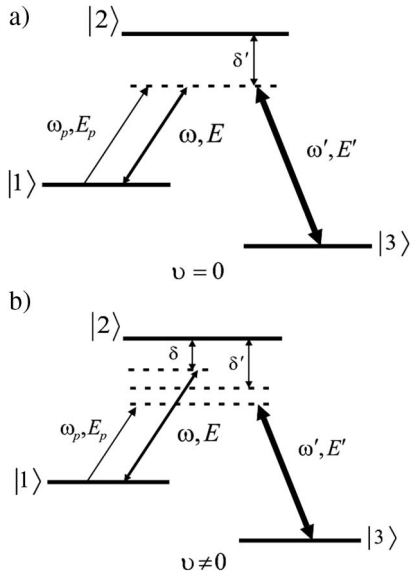

Fig. 3. Explanation for the EIT signal. (a) For the zero group-velocity atoms, the pump field and the probe field have the same frequency. Both of the control-probe fields and the control-pump fields satisfy the EIT condition. (b) For other atoms, the frequencies of the three fields are different.

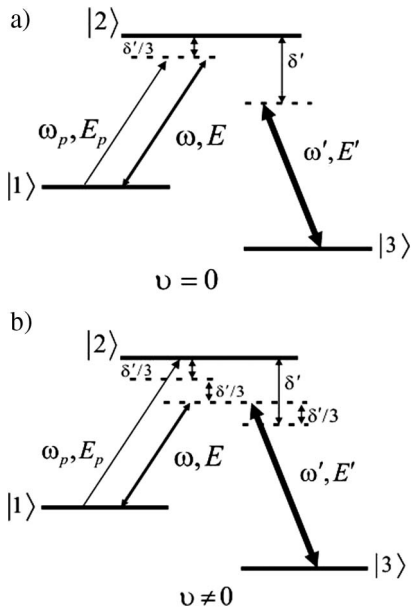

Fig. 4. Explanation for the EIA signal. (a) For the zero group-velocity atoms, the pump field and the probe field have the same frequency. There is no special process taking place. (b) For the atoms with the velocity $3c\delta'/\omega_p$, the pump field and the control field satisfy the EIT condition, and the probe field is absorbed by these atoms.

shown in Fig. 4(b). Since $\chi' \rangle \chi$, the atom population in level $|1\rangle$ is larger than that in level $|3\rangle$. The probe field interacts with these atoms and is absorbed by them, and then the EIA signal is observed. If the probe and the pump field travel with other detuning, there is no EIA signal. Because when the control field and the pump field satisfy the EIT condition, the probe field is not resonant with the atoms. When the probe field is resonant with some velocity group atoms, the control field and the pump field do not satisfy the EIT condition any more. This is the reason why EIT and EIA peaks have a fixed frequency relation.

From the above discussion, it is known that the EIA is induced by the population transfer due to the EIT process for some nonzero group-velocity atoms, and it takes place at both frequencies. The difference is the roles of the pump field and the probe field.

The Doppler-induced simultaneous EIT and EIA are experimentally observed. The sketch of the experimental setup is shown in Fig. 5. A 5 cm long, 2.5 cm diameter cell is filled with natural abundance rubidium without the buffer gas being filled. The cell is heated to 65°C. DL1 and DL2 are two commercial external-cavity diode lasers (TOPTICA DL100), which generate light with a wavelength of 795 nm. The control field derived from DL2 couples the transition $5S_{1/2}$, $F = 1 \rightarrow 5P_{1/2}$, $F' = 2$ of ^{87}Rb. It travels through the rubidium cell with the power ~10 mW and is blocked to avoid entering into the photo detector. The light from DL1 is divided into two beams by a 1:9 beam splitter. The strong beam acts as the pump field, which couples the transition $5S_{1/2}$, $F = 2 \rightarrow 5P_{1/2}$, $F' = 2$. It travels along the opposite direction with the power at 6 mW. The weak beam travels along the direction of the control field, which acts as the probe field and is detected by a large area photo detector (New Focus 2031). The signal is recorded by a digital oscilloscope (Tektronix TDS 2014B). The angle between the probe field and other fields is smaller than 2°.

The experimental results are shown in Fig. 6. The frequency of DL1 is scanned from the $5S_{1/2}$, $F = 2 \rightarrow 5P_{1/2}$, $F' = 1$ transition to the $5S_{1/2}$, $F = 2 \rightarrow 5P_{1/2}$, $F' = 2$ transition. The pump field and the probe field constitute a typical setup for the saturated absorption spectrum. So, it could find the saturated absorption spectrum of the $5S_{1/2}$, $F = 2 \rightarrow 5P_{1/2}$, F' transition in Fig. 6(a). The control field is red detuned from the transition $5S_{1/2}$, $F = 2 \rightarrow 5P_{1/2}$, $F' = 2$, and the detuning is about 350 MHz. There are two EIA signals in the spectrum, which correspond to the different δ' from the excited states $F' = 1$ and $F' = 2$, respectively. This result has been predicted in Fig. 2. In Fig. 6(b), the excited state $F' = 2$ is defined as the level $|2\rangle$. The ratio of the detuning of the

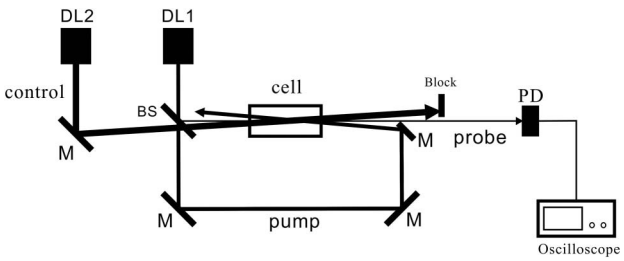

Fig. 5. Experimental setup for Doppler-induced simultaneous EIT and EIA. M, mirror; BS, 1:9 beam splitter; PD, photo detector.

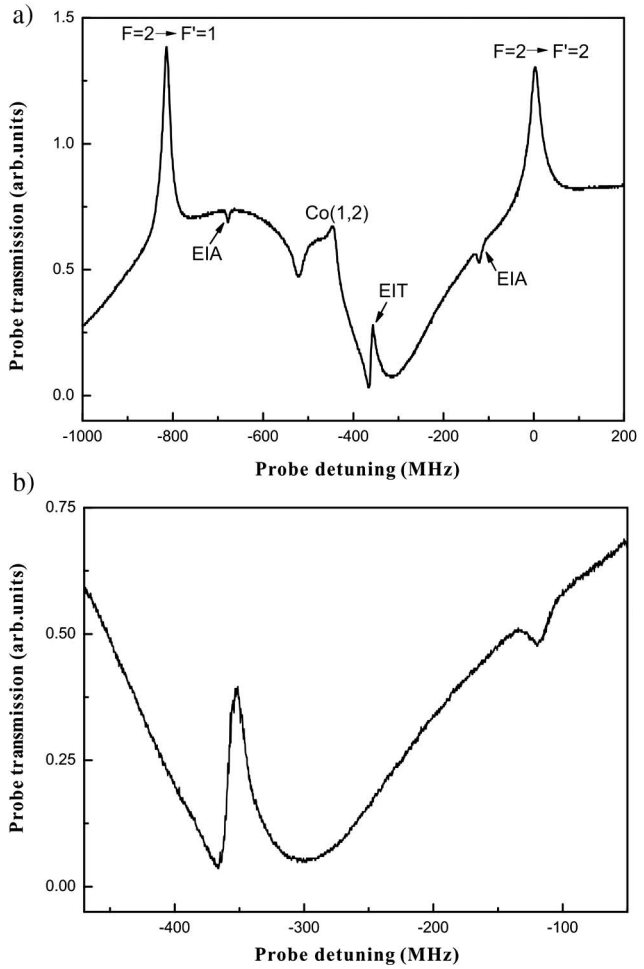

Fig. 6. Experimental results. (a) $F = 2 \rightarrow F' = 1$ and $F = 2 \rightarrow F' = 2$ are the saturated absorption signals of the transition $5S_{1/2}, F = 2 \rightarrow 5P_{1/2}$, $F' = 1$ and $F' = 2$, respectively. Co(1,2) is the crossover signal. (b) Simultaneous EIT and EIA signal. The ratio of the detuning of the probe field for the EIA signal to that for the EIT signal is 1:3.

probe field for the EIA signal to that for the EIT signal is 1/3, which is coincident with the analysis above.

In conclusion, Doppler-induced simultaneous EIT and EIA are investigated in a three-level lambda system. The phenomenon is analyzed theoretically and observed experimentally. The EIA signal arises due to the population transfer by the EIT process. The Doppler shifts make the roles of the three fields interacting with a hot atomic medium different for different velocity group atoms. It is an example of investigating the influence of the Doppler effect on quantum coherence.

This work was supported by the National Natural Science Foundation of China (No. 61475139), the National Basic Research Program of China (No. 2013CB329501), the National High Technology Research and Development Program of China (No. 2013AA063901), and the Fundamental Research Funds for the Central Universities (No. 2017FZA3005). We are greatly indebted to Xunming Cai and Jianqi Shen for the beneficial discussion and support in this work.

References

1. M. Fleischhauer, A. Imamoglu, and J. P. Marangos, Rev. Mod. Phys. **77**, 633 (2005).
2. G. Alzetta, A. Gozzini, L. Moi, and G. Orriols, Nuovo Cimento Soc. Ital. Fis. B **36**, 5 (1976).
3. A. Lezama, S. Barreiro, and A. M. Akulshin, Phys. Rev. A **59**, 4732 (1999).
4. J. Vanier, A. Godone, and F. Levi, Phys. Rev. A **58**, 2345 (1998).
5. S. Knappe, V. Shah, P. D. D. Schwindt, L. Hollberg, and J. Kitching, Appl. Phys. Lett. **85**, 1460 (2004).
6. I. Novikova, D. F. Phillips, A. S. Zibrov, and R. L. Walsworth, Opt. Lett. **31**, 622 (2006).
7. I. Novikova, D. F. Phillips, A. S. Zibrov, and R. L. Walsworth, Opt. Lett. **31**, 2353 (2006).
8. M. Fleischhauer and M.O. Scully, Phys. Rev. A **49**, 1973 (1994).
9. V. I. Yudin, A. V. Taichenachev, Y. O. Dudin, V. L. Velichansky, and A. S. Zibrov, Phys. Rev. A **82**, 033807 (2010).
10. N. Ram, M. Pattabiraman, and C. Vijayan, Phys. Rev. A **82**, 033417 (2010).
11. L. V. Hau, S. E. Harris, Z. Dutton, and C. H. Behroozi, Nature **397**, 594 (1999).
12. C. Liu, Z. Dutton, C. H. Behroozi, and L. V. Hau, Nature **409**, 490 (2001).
13. Y. Lee, H. J. Lee, and H. S. Moon, Opt. Express **21**, 22464 (2013)
14. M. S. Shahriar, G. S. Pati, R. Tripathi, V. Gopal, and M. Messall, Phys. Rev. A **75**, 053807 (2007).
15. I. Ben-Aroya and G. Eisenstein, Opt. Express **19**, 9956 (2011).
16. G. S. Pati, M. Salit, K. Salit, and M. S. Shahriar, Opt. Express **17**, 8775 (2009).
17. B. Luo, Y. Liu, and H. Guo, Opt. Lett. **35**, 64 (2010).
18. M. M. Hossain, S. Mitra, P. Poddar, C. Chaudhuri, and B. Ray, J. Phys. B: At. Mol. Opt. Phys. **44**, 115501 (2011).
19. G. Q. Yang, P. Xu, J. Wang, Y. Zhu, and M. S. Zhan, Phys. Rev. A **82**, 045804 (2010).
20. J. Wang, Y. Zhu, K. J. Jiang, and M. S. Zhan, Phys. Rev. A **68**, 063810 (2003).
21. K. Wang, W. Zhang, Z. Zhou, M. Dong, S. Shi, S. Liu, D. Ding, and B. Shi, Chin. Opt. Lett. **15**, 060201 (2017).
22. L. Jin, S. Gong, Y. Niu, and S. Jin, Chin. Opt. Lett. **4**, 252 (2006).
23. H. Zhou, S. Che, P. Zou, Y. Han, and D. Wang, Chin. Opt. Lett. **15**, 081401 (2017).
24. P. R. Berman and X. Xu, Phys. Rev. A **78**, 053407 (2008).